Damage assessment on building structures subjected to the recent near-fault earthquake in Lorca (Spain)

J. Donaire-Avila, A. Benavent-Climent, A. Escobedo, E. Oliver-Saiz, A.L. Ramírez-Márquez
Department of Structural Mechanics and Hydraulic Engineering. University of Granada, Spain.

M. Feriche
Andalusian Institute of Geophysics and Earthquake Disaster Prevention. University of Granada, Spain.

SUMMARY:
The city of Lorca (Spain) was hit on May 11th 2011 by two consecutive earthquakes with 4.6 and 5.2 Mw respectively, causing casualties and important damage in buildings. Lorca is located in the south-east region of Spain and settled on the trace of the Murcia-Totana-Lorca fault. Although the magnitudes of these ground motions were not severe, the damage observed was considerable over a great amount of buildings. More than 300 of them have been demolished and many others are being retrofitted. This paper reports a field study on the damage caused by these earthquakes. The observed damage is related with the structural typology. Further, prototypes of the damaged buildings are idealized with nonlinear numerical models and their seismic behavior and proneness to damage concentration is further investigated through dynamic response analyses.

Keywords: Lorca earthquake, damage concentration, seismic input energy, field study, infill panels.

1. INTRODUCTION

Lorca is a city settled along the Murcia-Totana-Lorca fault. This is a very active seismic zone located in the south-east region of Spain, on the edge of the European and African plates. Therefore, it is included in the Mediterranean basin which is an area with moderate seismicity. Historically, numerous earthquakes have occurred which have been measured based on the descriptions provided by people of the damage caused in buildings. Last May, 11th 2011, two new earthquakes hit the city of Lorca. The second one (mainshock in this case), was the strongest ever registered with accelerometers in Spain reaching a peak ground acceleration (PGA) of 0.36g (g is the acceleration of gravity). This series of earthquakes prompted a great amount of damage in buildings, injuries and also deaths. The PGA established by the current Spanish seismic code, NCSE-02 (Ministerio Fomento 2003) for Lorca is 0.11g, that is, less than one third the measured PGA. It is worth emphasizing that particularly severe damage was observed in historical constructions (heritage of Lorca) and moderns two-five stories building.

Most of the buildings damaged by Lorca earthquake used structural systems belonging to two commonly used typologies in Spain: reinforced concrete (RC) frame structures with wide beams supporting one-way joists, and RC waffle flat slabs supported by RC columns. Both systems have been widely used to withstand both gravity and lateral seismic loads, although it is not recommended in many international seismic codes, such as ACI (ACI Committee 318-08 2008). In Spain, the former seismis code PDS-74 (Ministerio de Obras Publicas 1974) did not provide any provision nor limitation on the use of wide beams or waffle flat slabs as earthquake resistant structural system. Later, the Spanish seismic code NCSE-94 (Ministerio de Obras Publicas 1995), banned the use of RC frames with wide beams or waffle flat plates in seismic areas with design acceleration a_c larger than 0.16g, and limited their strength reduction factor μ_{code} to 2 in other cases (i.e. a_c<0.16g). Here μ_{code} is a ductility coefficient defined by Eqn. 1.1:

$$\mu_{code} = \frac{\delta_u}{\delta_y} \tag{1.1}$$

Where δ_u is the ultimate displacement of the top floor of the structure and δ_y the yield displacement. The current Spanish seismic code NCSE-02 (Ministerio Fomento 2003) has removed the limitation on the use of RC frames with wide beams or waffle flat plates in regions with $a_c \geq 0.16g$ but adding new requirements on the size and distribution of the reinforcing bars on the wide beam. The limitation $\mu_{code}=2$ has been kept. The permissibility of the Spanish code and economic reasons (i.e. they are cheaper that other solutions) explain the wide use of these structural systems in the city of Lorca, although past research has emphasized their shortcomings as earthquake resistant system (i.e. limited energy dissipation capacity, large flexibility etc.).

The objective of this paper is to discuss, from field post-earthquake observations and the results of numerical analyses, the seismic behaviour of RC frame structures with wide beams seriously affected by the Lorca earthquake of May 2011. The distribution of the damage among the stories and the extra-supply of input energy in these structures are discussed in relation with the provisions of current Spanish seismic code and past research. The study focusses on buildings built in the last two decades, that were expected to behave reasonably well since they have been designed according to modern codes. To this end, two 4-story prototypes have been designed, following different codes in force in the last two decades in Spain. Two chronological windows have been set. The first window is from year 1994 to 2002, when the RC and seismic codes in force were EH-91 (Ministerio de Obras Publicas y Transportes 1991) and NCSE-94 (Ministerio de Obras Publicas 1995) respectively. The second window is from 2003 to 2008 and the RC and seismic codes in force at that time were EH-98 (Ministerio Fomento 1998) and NCSE-02 (Ministerio Fomento 2003). The role of claddings and masonry infill panels (commonly built with solid bricks) in shafts lift-stairs have being taken into account. Also, the presence of wide openings in facades (shop windows) and clear zones of the ground floor have been considered. Prototypes with and without infill panels have been modelled to run non-linear dynamic time history analysis. In these analyses, the two main events of the series of earthquakes occurred in Lorca in May, 11 2011 have been consecutively merged and considered as a single ground motion. The results of the numerical analyses have been compared with the damage observed in the buildings most severely damaged (and later demolished) in a field post-earthquake investigation.

2. MURCIA-TOTANA-LORCA FAULT AND EARTHQUAKES OF MAY 2011

The series of earthquakes occurred in Lorce in May 11, 2011 are attributed to the Murcia-Totana-Lorca fault (IGME 2011;Vissers & Meijninger 2011), a major 80 km long fault that runs close to the city centre, which was previously recognized as being active and having oblique reverse kinematics in this sector. From a seismological point of view, the 2011 earthquake was not an outstanding event in its regional context. In Murcia, three recent earthquakes with Mw=4.8, Mw=5.0 and Mw=4.8 occurred in 1999, 2002 and 2005, respectively (Mancilla et al. 2002).The 2011 Lorca earthquake, however, was very shallow and affected a highly populated urban area of nearly 92.000 inhabitants.

The series of two earthquakes with Mw=4.6 and Mw=5.2, respectively, had hypocenters less than 5 km depth at the edge NW of the city of Lorca. The station located on rock at a distance of 4 km from the epicentres registered peask ground accelerations of PGA=0.27g and PGA=0.36g, respectively. Both shocks reached VI and VII intensities (EMS), respectively, in Lorca, although some soil movement parameters such as Arias and Spectral intensity, suggest a maximum intensity of VIII. Moreover, directivity effects and soft soil influence show different levels of intensity according to the damage distribution throughout the city.

It is worth emphasizing that meaningful duration of the mainshock (time between 5% and 95% of Arias Intensity) was 0.935 seconds. This is an extremely small value which indicates that the energy input to the structures was supplied in a very short period of time, typical of the near fault source. This feature explains, at least partially, the severe damage observed in many structures.

3. DESCRIPTION OF THE DAMAGES IN BUILDINGS OF LORCA

Despite of low magnitude of the mainshock, damage in buildings has been widespread: nearly 80% of the buildings of Lorca have been affected with different levels of damage. According to the data provided by the Lorca council, 6416 of the 7852 buildings of the city were checked, and the observed damage measured with the EMS-98 scale was distributed as follows: 4035 (level 2), 1328 (level 3), 689 (level 4) and 329 (level 5) which collapsed or were demolished after the earthquake.

Two-story buildings were the mostly affected (5376 buildings, i.e. 68%), as well as old buildings belonging to architectural heritage. Moreover, 2212 (28%) buildings having from 3 to 5 stories were affected with different degrees of damage. The rest of damaged buildings (264, i.e. 4%) had more than 5 stories and experienced minor damage.

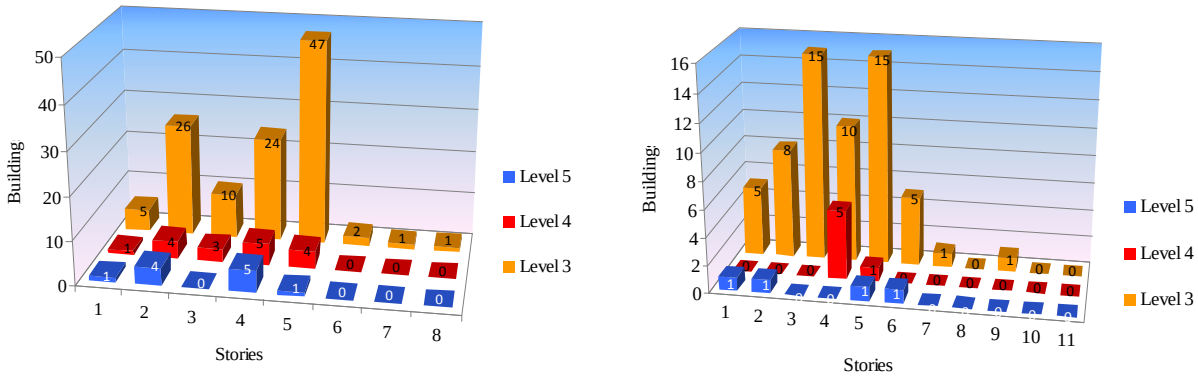

Figure 3.1. Number of damaged buildings with level greater than 2: (a) 1994-2002; (b) 2003-2008

In the two periods of interest in this paper, 1994-2002 and 2003-2008, the number of damage buildings was 755 and 373, respectively. Figure 3.1 shows the number of buildings with damage level greater than 3 in these two periods of time. It can be observed that there is an important number of buildings with severe structural and non-structural damages that have been designed following recent seismic codes. Two prototype RC frame structures with masonry infill walls with 4 stories were selected to analyse through non-linear dynamic response analyses the damage on both the main structure and the masonry infill walls. It is worth emphasizing that a large number of buildings with 3-5 stories and wide openings in the ground floor were severely damaged exhibit a “soft-story” pattern, as shown later in Figure 7.2.

4. FRAME DIRECTION AND INPUT ENERGY SPECTRA

For seismic assessment purposes, the two prototypes have been oriented in the direction corresponding to the highest spectral values of the input energy. This orientation is considered the worst scenario for the building from the point of view of energy dissipation demand. To determine the aforementioned direction, both NS and EW horizontal components of the accelerogram have been projected over a set of directions obtaining the accelerogram corresponding to each one. Finally, their energy input spectra for ξ=0.05, where ξ is the fraction of critical damping, have been calculated and expressed in form of equivalent velocity V_E defined by:

$$V_E = \sqrt{\frac{2 \cdot E}{M}} \tag{4.1}$$

Where E is the input energy and M the total mass of the building. The energy input spectra obtained in this way for different directions are shown in Figure 4.1. The highest spectral values were obtained along the N23ºW direction and have been plot separately in Figure 4.1.b, for the first (I) and second (II) shocks. The energy spectra of Figure 4.1.b were used in this paper to determine the input energy introduced in the prototypes investigated. In Figure 4.1.b a bilinear curve identified by MS is plotted which represents the design energy input spectra proposed by Benavent-Climent et. al for Spain in past

studies (Benavent-Climent et. al, 2002).

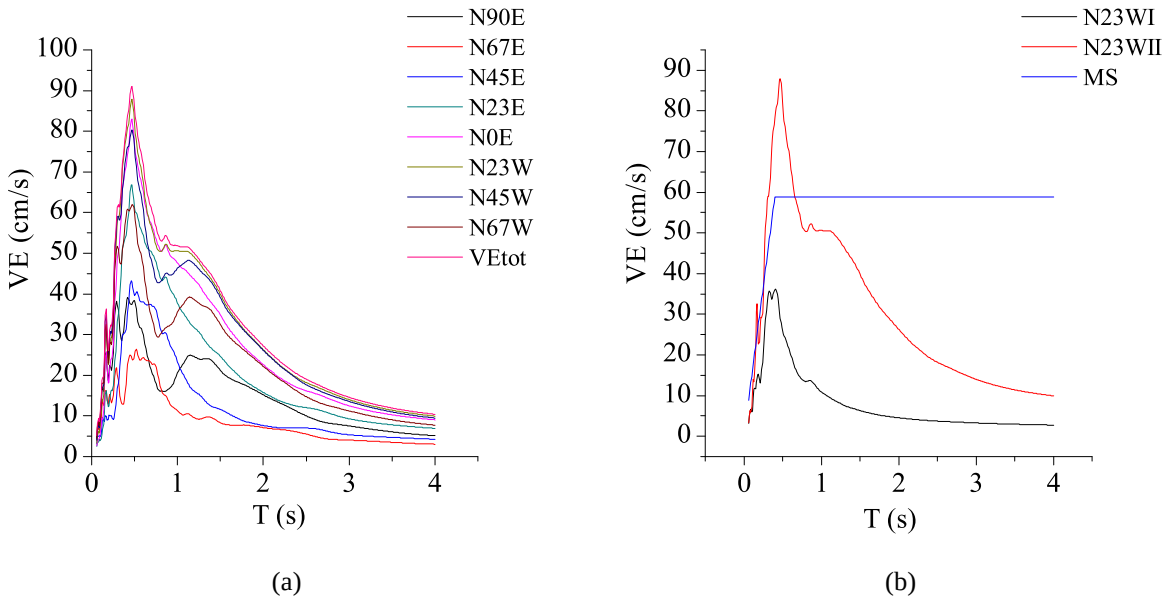

(a) (b)

Figure 4.1. Input Energy spectra for different directions (II shock) (a); and spectra with highest values (b).

5. PROTOTYPES AND NUMERICAL MODELS

5.1. Design of prototypes

The two prototypes considered in this paper and referred to as P1 and P2 hereafter, are four-story structures designed according to Spanish Standards with the software Tricalc (Artec S.A. 2010). As indicated in section 2, each of them was calculated following the codes in force in each period of time, that is, for the period 1994-2002 the EH-91 and NCSE-94 codes were considered; and for the period 2003-2008 the EH-98 and NCSE-02 codes were used. Figure 5.1 shows three of the five frames that constitute the prototypes. The other two frames are identical to those shown in Figure 5.1.a and Figure 5.1.b (i.e. the structure is symmetric). Also shown in the figure is the configuration of the infill walls.

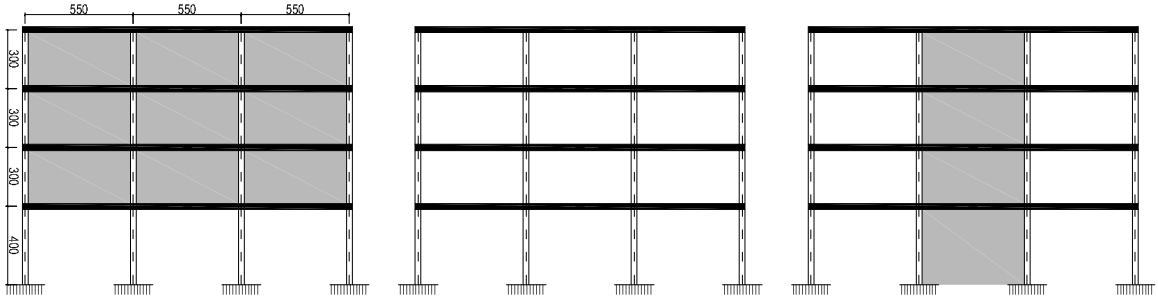

(a) (b) (c)

Figure 5.1. Different frames of the prototypes. (a) exterior, (b) interior and (c) central frames

The main difference between the prototypes P1 and P2 is the yield strength of the concrete. In the first prototype (P1) a nominal strength of 17.5MPa was used whereas in the second one (P2), the minimum value of 25MPa allowed by EH-98 code was used. In both prototypes the yield strength of the steel used as reinforcement was 400MPa, as was the most common practice at that time. The same gravity loads were considered in both prototypes: (a) self-weigh of the floor plus dead loads: 4.25 kN/m^2; (b) self-weigh of the roof plus dead load: 3 kN/m^2; and (c) live loads 3.2 kN/m^2. Few differences can be found in sections. Column's size ranged from 25x25 cm up to 40x40cm. Beam's size ranged from *b*x*h*=40x30 cm to 70x30cm, where *b* is the width of the wide beam and *h* is the depth. As for the seismic loads, a modal spectral analysis was carried out and a ductility factor μ_{code} =2 was adopted in

both prototypes. Similar PGA (0,11g) and soil conditions (type II, medium-stiff to stiff soil) were used for designing both prototypes.

5.2. Numerical models. Frames and infill panels

Non-linear numerical models were defined using frame elements with lumped plastic hinges at the ends of the columns and beams, following the geometry and reinforcement obtained in design (section 5.1). The program IDARC version 6.1 was used for both pushover and non-linear time history analysis. Plastic hinges were modelled using non-linear spring elements. In the case of beams, the moment-curvature envelope curve was idealized with a bilinear model and calibrated with the experimental results of past research (Benavent-Climent 2007;Benavent-Climent, Cahís, & Zahran R. 2009). For columns, the moment-curvature envelope curve was idealized using a trilinear model that took into account the moment-axial force interaction in the column. To characterize the hysteretic behavior of the masonry infill panels the Bouc-Wen modified model was adopted. The lateral yield strength and the initial lateral stiffness of the infill walls were taken from the previous laboratory test (Pujol et al. 2008). The results of these were used also to calibrate the Bouc-Wen modified model so that it captures relevant aspects of the cyclic behavior such as the degradation of lateral strength and stiffness and the pinching effect. Since a main objective of this work was to study the influence of the infill panels on the seismic behavior of the RC frames, two analyses were conducted for each prototype. In the first analysis, referred to as Pi-W the frame included infill walls. In the second analysis, referred to as Pi infill panels were not included (bare frame). Here the index *i* indicates the period of time to which the structure belongs. In the Pi-W cases, claddings were continuous among the stories except in the ground story where infill walls were absent (open ground story as shown in Figure 5.1). In all cases (Pi-W and Pi analyses) the infill panels that form the shaft lift-stairs were included in all stories (including ground floor).

5.3. Static response of each story throughout push-over analysis

Push-over analyses with displacement control were conducted using an inverse triangular distribution on each prototype building, with and without infill panels, in order to obtain the monotonic shear force versus inter-story curve of each story. In the Pi-W models, the infill panels work in parallel with the main RC frame, and it is possible to evaluate separately the contribution of each part (the bare frame and the infill walls) to the total lateral shear force of the story. The subscripts *w* and *rc* denote hereafter the contribution of the infill panels and bare RC frames, respectively. From the monotonic curves, the yield lateral strength Q_{yi}, the yield displacement δ_{yi}, and the ultimate displacement δ_{ui} are evaluated. To this end, a bilinear equivalent envelope was calculated by applying the Newmark & Hall's approach (Newmark & Hall 1982). For the bare RC frame δ_{ui} was determined as the displacement beyond which the lateral shear force decreases below 20% of the maximum value attained in the pushover curve. As for the infill panels, the δ_{ui} corresponding to a ductility factor of 3 (defined by Eqn. 5.1) was adopted (DolseK & Fajfar 2008). The corresponding values obtained are summarized in Table 5.1 and Table 5.2.

$$\mu_{i\max} = \frac{\delta_{ui} - \delta_{yi}}{\delta_{yi}} \tag{5.1}$$

The ductility factor μ_{imax} was calculated from the envelope curve Q_{yi}-δ_{yi} of each story for the bare RC frame and is shown in Table 5.1 and Table 5.2. Comparing the definitions given by Eqn. 1.1 and Eqn. 5.1 it is obvious that $\mu_{code}=\mu_{imax}+1$. As can be seen in Table 5.1 and Table 5.2, in some stories, $\mu_{imax}+1$ is slightly below the value (2) prescribed by the Spanish codes and adopted in section 5.1 for designing the prototypes.

Table 5.1. Static response of prototypes P1 and P1-W (push-over analyses)

	Prototype P1 (RC bare frames)					Prototype P1-W (frame with infill walls)			
Story	${}_{rc}\delta_{yi}$ *(mm)*	${}_{rc}\delta_{ui}$ *(mm)*	${}_{rc}\mu_{imax}$	${}_{rc}\mu_{imax}+1$	${}_{rc}Q_{yi}$ *(kN)*	${}_{w}\delta_{yi}$ *(mm)*	${}_{w}\delta_{ui}$ *(mm)*	${}_{w}\mu_{imax}$	${}_{w}Q_{yi}$ *(kN)*
1	24.91	39.89	0.60	1.60	1074	5.59	23.02	3	396
2	17.82	37.52	1.11	2.11	996	5.59	23.01	3	2775
3	17.72	36.71	1.07	2.07	778	5.72	23.05	3	2773
4	19.97	35.81	0.79	1.79	644	5.73	23.07	3	2772

Table 5.2. Static response of prototypes P2 and P2-W (push-over analyses)

	Prototype P2 (RC bare frames)					Prototype P2-W (frame with infill walls)			
Story	${}_{rc}\delta_{yi}$ *(mm)*	${}_{rc}\delta_{ui}$ *(mm)*	${}_{rc}\mu_{imax}$	${}_{rc}\mu_{imax}+1$	${}_{rc}Q_{yi}$ *(kN)*	${}_{w}\delta_{yi}$ *(mm)*	${}_{w}\delta_{ui}$ *(mm)*	${}_{w}\mu_{imax}$	${}_{w}Q_{yi}$ *(kN)*
1	17.61	33.08	0.88	1.88	886	5.84	22.98	3	380
2	21.96	36.18	0.65	1.65	819	5.72	23.01	3	2663
3	18.65	30.57	0.64	1.64	768	5.72	23.02	3	2663
4	13.19	26.32	1.00	2.00	497	5.71	23.01	3	2663

6. NON-LINEAR TIME HISTORY ANALYSIS

Non-linear time history analyses were carried out with the numerical models representing the prototype structures, with and without infill walls. It is worth emphasizing that in the design of the RC bare frames explained in sub-section 5.1 infill panels were not included as structural elements. However, the contribution of the infill walls to the lateral strength, stiffness and in general to the hysteretic behavior of the buildings has been included in the non-linear dynamic response analyses. All prototypes (Pi-W and Pi) were subjected to two accelerograms. The first one corresponds to the first shock occurred in Lorca in May 11, 2011. The second accelerogram was built by merging the two consecutive strongest ground motions recoded in Lorca in May 11, 2011. The first accelerogram served to study the damage and the change on the stiffness of the structures before being subjected to the strongest ground motion that occurred about 45 minutes later.

7. RESULTS

7.1. Influence of the infill panels on the stiffness of the RC frames

The main elastic period *T* of the prototypes P1 and P1-W was 1.43 and 0.73s, respectively. Infill panels reduced the period of the bare RC frame structures by 49%. On prototypes P2 and P2-W, the results were similar, with main periods equal to 1.48 and 0.70s. Table 7.1 summarizes the elastic period and lateral stiffness of each story.

Table 7.1. Stiffness and elastic fundamental periods of prototypes

	P1	P1-W	P2	P2-W
	T= 1.42 s	*T= 0.73 s*	*T= 1.48 s*	*T= 0.70 s*
Story	*k (kN/cm)*	*k (kN/cm)*	*k (kN/cm)*	*k (kN/cm)*
1	431	956	504	1012
2	559	5493	373	5093
3	439	5486	412	5200
4	322	5245	377	5297

7.2. Damage level after the first earthquake

The energy input spectrum of the first earthquake is lower than that of the second one, although the shapes are similar as shown in Figure 4.1.b. This implies that the energy input in all prototypes, with and without infill panels, are lower for the first than for the second shock. The results of the non-linear dynamic response analyses show minor damage after the first earthquake: cracking on the structural members at the ground floor level, inter-story drifts below the yield limit, and no damage on the infill panels.

7.3. Damage after the second earthquake

The second earthquake was responsible for the damage experienced by the structures. Input energy in all prototypes was extremely higher in after the second earthquake in comparison to the values after the first ground motion. Thus, hereafter only the data obtained from the prototypes subjected to the second earthquake will be discussed.

7.4. Energy dissipation

Dissipated energy on each story, E_h, was calculated for all prototypes. E_h was obtained by integrating

the story shear force Q_i versus inter-story displacement, Q_i-δ_i, of each story. Further, E_h was normalized by the product of Q_i and δ_i at yielding, Q_{yi} and δ_{yi}, by means of a cumulative plastic strain ratio η_i defined by:

$$\eta_i = \frac{E_h}{Q_{yi} \cdot \delta_{yi}} \tag{7.1}$$

The ratio η_i is a good indicator of the damage cumulated on the story i through the plastic strain reversals. A preferable seismic design should be aimed at attaining a uniform distribution of η_i among the stories. When the value of η_i is the same in all stories, the plastic strain energy is considered to have been dissipated in an optimal way (Akiyama H. 1985) and damage concentration has not occurred. Another relevant parameter μ_i can be obtained from the hysteretic curve Q_i-δ_{yi} of each story. μ_i represents in a non-dimensional form the maximum apparent (i.e. non-cumulative) plastic deformation of the story and it is defined as follows:

$$\mu_i = \frac{\delta_i - \delta_{yi}}{\delta_{yi}} \tag{7.2}$$

Here δ_i is the maximum inter-story displacement (in positive or negative domain) of the i-th story. The η_i/μ_i ratio is an important response parameter of the structure because it measures the efficiency of the systems in dissipating energy through plastic deformations. The larger the ratio η_i/μ_i is the better, because it means that the structure can dissipate large amounts of energy with small lateral displacements. Typically, η_i/μ_i is larger for far-fault earthquakes than for near-fault ones (Manfredi, Polese, & Cosenza 2003). Fig. 7.1.a shows the distribution of η_i for the prototypes P1 and P2 (without infill panels) and it can be seen that η_i is nearly constant. Table 7.2 summarizes the values of η_i, μ_i and the ratio η_i/μ_i. Prototype P1 developed a strong column-weak beam failure mechanism, while prototype P2 showed a collapse mechanism of the weak columns-strong beam type. Moreover, Fig. 7.1.b. shows that both prototypes P1 and P2 exhibit a nearly even distribution of δ_i, which is a direct consequence of the even distribution of η_i.

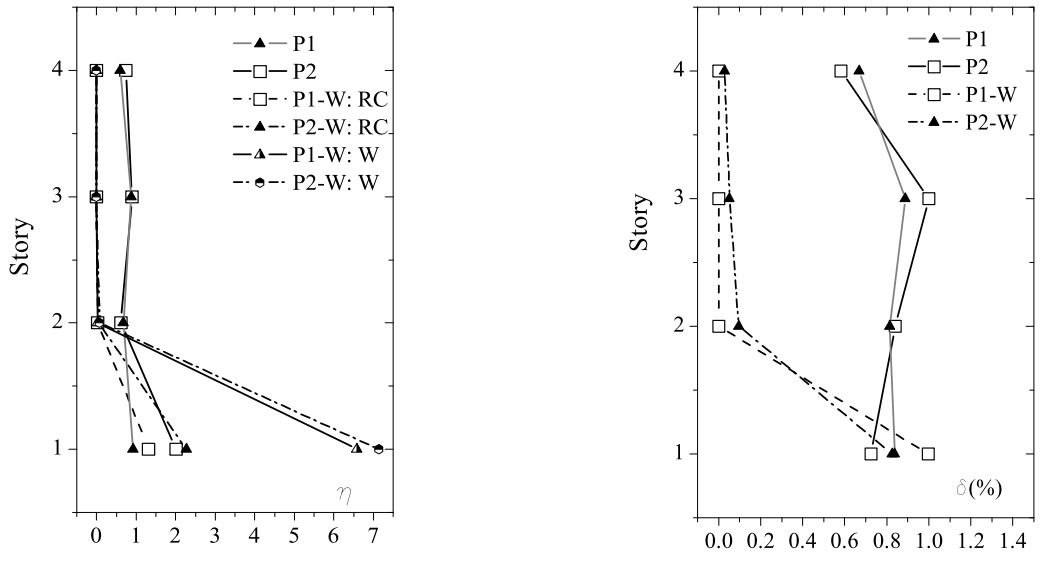

Fig. 7.1. Distribution of: (a) η_i in bare frames (P1, P2), in the frames of RC frames with infill panels (P1-W:RC and P2-W:RC), and in the infill walls of RC frames with infills (P1-W:W and P2-W:W); (b) inter-story drifts

Table 7.2. Dynamic response of prototypes without infill panels (dynamic response analyses)

	Prototype P1			Prototype P2		
Story	μ_i	η_i	η_i/μ_i	μ_i	η_i	η_i/μ_i
1	0.35	0.93	2.68	0.65	2.01	3.10
2	0.37	0.68	1.84	0.15	0.62	4.22
3	0.51	0.89	1.75	0.61	0.90	1.48
4	0.01	0.60	-	0.32	0.75	2.31

The dynamic response changes drastically when infill panels are included. In prototype P1-W and P2-W, the damage concentrated in ground floor and its collapse triggered off the collapse of the overall structure. The η_i distribution is shown Fig. 7.1.a and it is clearly seen the damage concentration of damage on the ground story. Infill panels that enclosed the shaft of the elevator and stairs of the ground floor collapsed and the plastic hinges at both ends of the columns of the ground level reached their ultimate capacity. A weak column-strong beam collapse mechanism developed at the ground level that jeopardized the stability of the overall building. Fig. 7.1.b shows the distribution of δ_i, where it can be seen that all plastic deformations concentrate on the ground floor while the upper part of the structure remains elastic with lateral inter-story drifts below 0.1%. This type of failure is commonly known as "soft story" failure, and it was observed in many buildings with open ground story and weak claddings after the Lorca earthquake as shown in Figure 7.2. This figure shows different views of the ground floor of a 4-story building built at the beginning of the current century.

Table 7.3. Dynamic response of prototypes with infill panels (dynamic response analyses)

	Prototype P1-W						Prototype P2-W					
	RC			W			RC			W		
Story	$_{rc}\mu$	$_{rc}\eta$	$_{rc}\eta/_{rc}\mu$	$_{w}\mu$	$_{w}\eta$	$_{w}\eta/_{w}\mu$	$_{rc}\mu$	$_{rc}\eta$	$_{rc}\eta/_{rc}\mu$	$_{w}\mu$	$_{w}\eta$	$_{w}\eta/_{w}\mu$
1	0.60	1.32	2.20	3.12	6.58	2.11	0.88	2.28	2.60	2.93	7.14	2.43
2	0.00	0.00	-	0.00	0.00	-	0.00	0.00	-	0.00	0.00	-
3	0.00	0.00	-	0.00	0.00	-	0.00	0.00	-	0.00	0.00	-
4	0.00	0.00	-	0.00	0.00	-	0.00	0.00	-	0.00	0.00	-

(a) (b)

Figure 7.2. Damage concentration on ground floor of a 4-story building after Lorca earthquake 2011).

Another relevant aspect of the dynamic response of the prototypes P1-W and P2-W is the distribution of the plastic strain energy (hysteretic energy) in each story between RC frame and the infill panels. Table 7.4 shows the plastic strain energy dissipated on each story by the infill walls, E_W, by the RC frames, E_{RC}, and the total hysteretic energy $E_h = E_{RC}+E_W$. In the ground story, which triggered off the collapse of the whole building, the plastic strain energy is dissipated mainly by RC structure. This is due mainly to the small amount of infill panels placed in this story (only those enclosing the shaft of the elevator and stairs). In the rest of the stories the amount of infill panels is larger and thus they are able to dissipate more energy. As the interstory drift in upper stories was very low, only infill panels could dissipate energy (2nd and 3rd story).

Table 7.4. Distribution of plastic strain energy in each story between infill panels and RC structure

	P1-W					P2-W				
Story	E_w kNmm	E_w/E_h (%)	E_{RC} kNmm	E_{RC}/E_h %	E_{Tot} kNmm	E_w kNmm	E_w/E_h %	E_{RC} kNmm	E_{RC}/E_h %	E_h kNmm
1	14579	29	35314	71	49893	15857	31	35616	69	51473
2	508	45	619	55	1127	1143	62	713	38	1856
3	40	100	0	0	40	21	100	0	0	21
4	8	100	0	0	8	5	100	0	0	5
TOTAL	15135	30	35933	70	51068	17026	32	36329	68	53355

7.5 Input Energy on prototypes

The energy that contributes to damage on a structure, E_D, is the sum of the elastic vibration energy and the hysteretic energy E_h summarized in Table 7.4. E_D can be expressed in terms of an equivalent velocity V_D defined with Eqn. 4.1 by replacing E with E_D. At the end of the ground motion the elastic vibration energy is very small in comparison to E_h and it can be neglected for the sake of simplicity. The plastic energy obtained from the dynamic non-linear analysis will be referred to as V_{DC}. The spectral values for V_D, referred to as V_{DSP} hereafter, can be obtained from the V_E spectrum of the main shock (N23ºWII) shown in Figure 4.1.b, by applying the following Eqn. 7.3 proposed by Akiyama (Akiyama H. 1985) where ξ is the fraction of damping.

$$(V_D/V_E)=1/(1+3\xi+1.2\xi^{0.5}) \quad (7.3)$$

Table 7.5 shows that V_{DC} is very close to V_{DSP} in all prototypes. It has been included in Fig. 4b the bilinear design energy input spectrum proposed for Spain by Benavent-Climent et al. (Benavent-Climent, Pujades, & López-Almansa 2002). From this spectrum the energy input in terms of equivalent velocity V_E was obtained and it is referred to as V_{EMS} in Table 7.5. From V_E, the energy that contributes to damage in terms of the equivalent velocity V_D was calculated with Eqn. 7.3 and it is referred in Table 7.5 as V_{DMS}. It can be seen in Table 7.5 that the values of V_{DMS} are higher than V_{DC} and V_{DSP} for the range of periods of the prototypes analyzed. However, in the range of periods 0.25-0.69 s the opposite situation arises because in that window of periods the energy input spectrum of Lorca earthquake is higher than the design spectrum proposed by Benavent-Climent et at.

Table 7.5. Input energy by the ground motion on the prototypes

Prototype	T_1 (sec)	V_{DC} (cm/s)	V_{DSP} (cm/s)	V_{EMS} (cm/s)	V_{DMS} (cm/s)
P1	1.43	32	38	59	41
P1-W	0.73	30	29	59	41
P2	1.48	33	39	59	41
P2-W	0.70	31	29	59	41

8. CONCLUSIONS

A numerical study on the seismic behavior of RC frame structures with wide beams, with and without masonry infill walls, was conducted to clarify the damage exhibited by this type of structural systems during the recent earthquake occurred in Lorca (Spain) in May 11th, 2011. A large number of buildings of this type suffered severe damage (level 4-5 in the EMS scale) or even collapsed after this earthquake. To this end, several prototypes representing 4-story RC frame structures were designed according to Spanish codes in force in two different periods of time in Spain: 1994-2000 and 2000-2008. The objective was to identify differences on the seismic response of the structures designed in these two periods of time, and to investigate quantitatively the influence of the uneven distribution of infill walls along the height of the building; more precisely, the effect open zones (lack of infill walls) at the ground level on damage concentration. Non-linear time history analyses conducted with numerical models which restoring force characteristics and hysteretic laws were calibrated with past experimental research.

The prototypes without infill panels, P1 and P2, showed an even distribution of damage among the stories in terms of a cumulative plastic strain energy ratio η_i. However, the prototype P1 designed with the Spanish codes in force from 1994 to 2000 exhibited a strong column-weak beam collapse mechanism, while the prototype P2 designed with the Spanish codes in force in the period 2001-2008 developed a weak column-strong beam behaviour and a slightly higher damage concentration in ground floor than prototype P1. However, neither of both prototypes collapsed.

Infill panels were included in the prototype structures P1 and P2, and two new prototype buildings referred to as P1-W and P2-W were developed. The two exterior frames of prototypes P1-W and P2-W were provided with masonry infill wall in all stories except in the ground floor. Masonry infill wall enclosing the shaft of the elevator and stairs were considered in all stories of prototypes P1-W and P2-W (including the ground floor). The results of non-linear dynamic response analyses showed a clear

damage concentration in ground floor the triggered off the collapse of the whole building. In both cases, the lateral stiffness of the ground floor was markedly smaller than in the rest of stories. Damage at the ground floor was intensified by the increase of input energy associated with the shift of the fundamental period of the structure caused by the addition of infill walls. Therefore, the presence of infill panels with a non-uniform distribution over the height of the building makes the building very prone to damage concentration, and jeopardizes the overall seismic resistance of the building unless the story where the plastic strain energy is expected to concentrate is specially prepared to dissipate the energy dissipation demand imposed by the earthquake. One effective solution for improving the energy dissipation capacity of a given story and preparing it for damage concentration consist on installing hysteretic dampers (positive use of damage concentration effects). Hysteretic dampers can be used in both new construction or for seismic retrofitting of existing buildings.

REFERENCES

ACI Committee 318-08 2008, *Building code requirements for structural concrete (ACI 318-08) and commentary*, American Concrete Institute edn.

Akiyama H. 1985, *Earthquake resistant limit-state for buildings* University of Tokyo Press, Tokyo.

Artec S.A. TRICALC. [7.1]. 2010. Computer Program

Benavent-Climent, A. 2007, "Seismic behavior of RC wide beam-column connections under dynamic loading", *Journal of Earthquake Engineertin*, **vol. 11**, pp. 493-511.

Benavent-Climent, A., Cahís, X., & Zahran R. 2009, "Exterior wide beam-column connections in existing RC frames subjected to lateral earthquake loads", *Engineering Structures*, **vol. 34**, pp. 1414-1424.

Benavent-Climent, A., Pujades, L. G., & López-Almansa, F. 2002, "Design energy input spectra for moderate-seismicity regions", *Earthquake Engineering & Structural Dynamics*, **vol. 31**, pp. 1151-1172.

DolseK, M. & Fajfar, P. 2008, "The effect of masonry infills on the seismic response of a four-storey reinforced concrete frame_ a deterministic assesment", *Engineering Structures*, **vol. 30**, pp. 1991-2001.

IGME 2011, *Informe Geológico Preliminar del Terremoto de Lorca del 11 de Mayo del año 2011, 5.1 Mw*, Instituto Geológico y Minero de España.

Mancilla, F., Ammon, C. J., Herrmann, R. B., & Morales, J. 2002, "Faulting parameters of the 1999 Mula earthquake, southeastern Spain", *Tectonophysics*, **vol. 354**, pp. 139-155.

Manfredi, G., Polese, M., & Cosenza, E. 2003, "Cumulative demand of the earthquake ground motions in the near source", *Earthquake Engineering & Structural Dynamics*, **vol. 32**, pp. 1853-1865.

Ministerio de Obras Publicas y Transportes 1991, *Instrucción para el proyecto y la ejecución de obras de hormigón en masa o armado (EH-91)* Centro Publicaciones-Ministerio Obras públicas y Transportes.

Ministerio de Obras Publicas, T. y. M. A. 1974, *Norma Sismorresistente P.D.S.-1/1974.* Centro de Publicaciones.

Ministerio de Obras Publicas, T. y. M. A. 1995, *Norma de Construcción Sismorresistente, Parte General y de Edificación (NCSE-94)* Servicio de Publicaciones.

Ministerio Fomento 1998, *Instrucción de Hormigón Estructural (EHE-98)* Centro Publicaciones-Ministerio Fomento.

Ministerio Fomento 2003, *Norma de Construcción Sismorresistente: Parte general y edificación (NCSE-02)*, 2004 edn, Centro Publicaciones-Ministerio Fomento-España.

Newmark, N. M. & Hall, W. J. 1982, *Earthquake Spectra and Design*, Berkeley, California: Earthquake Engineering Research Institute.

Pujol, S., Benavent-Climent, A., Rodríguez, M. E., & Smith-Pardo, J. P. "Masonry Infill Walls: an effective alternative for seismic strengthening of low-rise reinforced concrete building structures", in *14th World Conference on Earthquake Engineering*.

Vissers, R. L. M. & Meijninger, B. M. L. 2011, "The 11 May 2011 Earthquake at Lorca (SE Spain) viewed in a structural-tectonic context", *Solid Earth*, **vol. 2**, pp. 199-204.